Climate-sensitive models of tree mortality based on lifetime analysis and irregular permanent-plot remeasurements

Mathieu Fortin[1,*], José Riofrío[2], Lara Climaco de Melo[2], Muhammad Waseem Ashiq[3], Mahadev Sharma[4], Christina Howard[2], and Bianca N. I. Eskelson[2]

[1]Canadian Wood Fibre Centre, Canadian Forest Service, Natural Resources Canada, Ottawa, ON K1A 0E4, Canada

[2]Department of Forest Resources Management, The University of British Columbia, Vancouver, BC V6T 1Z4, Canada

[3]Science and Research Branch, Ontario Ministry of Natural Resources, Peterborough, ON K9J 3C7, Canada

[4]Ontario Forest Research Institute, Ontario Ministry of Natural Resources, Sault Ste Marie, ON P6A 2E5, Canada

[*]Corresponding author: mathieu.fortin@nrcan-rncan.gc.ca

December 9, 2024

Abstract

Climate change has driven forest growth modellers to develop different climate sensitivity implementations (CSI) for their models. Among others, a model can rely on annual climate variables or average climate variables, such as 30-year normals. The novelty of this study was to develop a framework based on lifetime analysis to enable annual or average CSI in empirical models of tree mortality. Using this framework, we compared models of individual tree mortality based on an annual CSI with similar models relying on two average CSIs, one using interval-averaged climate variables, and the other, 30-year normals. We fitted these models to permanent-plot data of eight species in Ontario and tested the effects of summer and winter temperature as well as spring and summer precipitation in the models.

Our results showed that the annual CSI was not superior to the average CSIs, but could be a valid alternative for some species. Warmer winter temperature was detrimental to the survival of *Betula papyrifera*, *Picea glauca*, and *Pinus strobus*, whereas greater spring and summer precipitation resulted in greater mortality occurrence for *Picea mariana*, *Pinus banksiana*, and *Populus tremuloides*. In most cases, the effects of climate variables were contrary to our initial hypotheses. We conclude that the effects of climate on tree mortality occurrence interact with other factors such as species distribution and ecophysiology.

Keywords. Lifetime analysis; Individual tree mortality; Climate sensitivity; Temperature; Precipitation; Hazard function

1 Introduction

Over the last two decades, forest growth modellers have strived to make their models climate sensitive in order to better predict the impacts of climate change. Whether they are empirical, process-based, or hybrid, many forest growth models now have a certain degree of sensitivity to climate. In North America for instance, a climate-sensitive version of the Forest Vegetation Simulator (FVS) is now available (Crookston et al., 2010) and the Mixedwood Growth Model (MGM) used in western Canada has climate-sensitive components of mortality and diameter increment (Cortini et al., 2017; Oboite and Comeau, 2021).

Metsaranta et al. (2024) defined four levels of climate sensitivity implementation (CSI) in forest growth models used in Canada:

1. No climate sensitivity, which assumes climate remains approximately equivalent to what it was in the data used to fit the model;

2. An indirect CSI through an explanatory variable, typically a climate-sensitive site index (e.g., Crookston et al., 2010; Sharma, 2021);

3. An average CSI, when some model components include 30-year normals or interval-averaged climate variables in their equations (e.g., Cortini et al., 2017; Fortin et al., 2023);

4. An annual CSI, when some model components include annual or intra-annual climate variables (e.g., Larocque et al., 2011).

The same authors found that many empirical forest growth models in Canada benefit from an indirect or average CSI, but none of them implements annual climate variables. This is surprising given the fact that most of these Canadian models predict growth on an annual basis (Metsaranta et al., 2024).

Typically, empirical forest growth models are fitted to permanent-plot data. However, permanent plots are rarely remeasured on an annual basis; remeasurements are usually car-

ried out on longer, and often irregular, time intervals, ranging from 5 to 15 years. The repeated measurements of trees provide the information to model the basic components of stand growth: mortality, survivor growth, and ingrowth (Vanclay, 1994, p. 9). For each one of these three components, the response variable can be annualized (e.g., Li et al., 2011; Cortini et al., 2017; Oboite and Comeau, 2021). However, the climate variables that have an effect on tree mortality, survivor growth, and ingrowth can hardly be expressed on an annual basis in regular statistical regression. As a matter of fact, this is only possible when the remeasurement interval is strictly regular across the plots, e.g., every 5 years. It then requires a parameter for each combination of climate variable and year, which increases the complexity of the model.

In practice, irregular remeasurement intervals imply that most empirical modellers have to implement climate sensitivity in their models through variables depicting the average climate, such as 30-year normals (Cortini et al., 2017) or interval-averaged climate variables (Fortin et al., 2023). However, the fact that average climate variables can hide extreme annual values cannot be overlooked (Oboite and Comeau, 2021). There could be a gain, both in model fit and biological realism, to consider annual climate variables in empirical forest growth models.

One component of growth models that can be expected to be climate sensitive is the mortality part. In most studies on the topic, mortality is modelled using logistic regression (e.g., Pretzsch et al., 2002; Dietze and Moorcroft, 2011; Cortini et al., 2017). While logistic regression can adapt to irregular remeasurement intervals, it cannot account for annual climate variables measured within these irregular intervals, since the number of model parameters would vary across the observations.

Statistical models designed for the analysis of lifetime data are also meant to predict the probability of occurrence of a particular phenomenon. Unlike logistic regression, lifetime models use the concept of hazard accumulation over time (Lawless, 2003). In forest growth modelling, there are a few examples of lifetime models applied to tree mortality

(e.g., Rose et al., 2006; Fortin et al., 2008; Hämäläinen et al., 2016; Neumann et al., 2017; Maringer et al., 2021). The hazard accumulation is done through a hazard function (Lawless, 2003, p. 10), which allows for time-varying explanatory variables. This hazard function could be the entry point of annual climate variables in a model of tree mortality. Interestingly, to the best of our knowledge, this approach has never been tested.

The main objective of this paper was to develop a framework based on lifetime analysis and to compare the performance of different CSIs in tree mortality models. Our hypothesis was that (H1) an annual CSI in empirical tree mortality models would provide a better fit compared with an average CSI based on 30-year normals or interval-averaged climate variables. To test this hypothesis, we fitted mortality models to eight major tree species in the province of Ontario, Canada.

A secondary objective was to improve our understanding of climate impacts on tree mortality in boreal and temperate forests in eastern Canada. Warm temperatures are known to affect the water balance of trees during the growing season and can eventually lead to greater mortality occurrence (Hartmann et al., 2022). However, warmer winter temperatures could be beneficial if cold is a limiting factor. For instance, Neumann et al. (2017) showed that warmer winter temperatures of the previous year were beneficial to the survival of European tree species in general. From a growth perspective, Huang et al. (2010) showed that radial growth of a few Canadian boreal tree species was greater after warmer winters. Consequently, we hypothesized that (H2) warmer summer temperatures are detrimental to tree survival, but that (H3) warmer winter temperatures favour tree survival. Precipitation increases the water availability and therefore, it contributes to the water balance of trees (Hember et al., 2017). Therefore, we also hypothesized that (H4) lower spring or summer precipitation is detrimental to tree survival.

2 Material and Methods

2.1 Statistical developments

Tree mortality can be modelled through a lifetime analysis approach, which is largely described in Lawless (2003). Let T be a random variable representing the exact time of death of an individual. The probability that this individual is dead at time t is $F(t) = \Pr(T \leq t)$. Equivalently, the probability that a tree survives until time t is the balance of probability, which is referred to as the survivor function $S(t) = 1 - F(t)$. The hazard function $h(w)$, which is a fundamental concept of lifetime models, represents the instantaneous rate of mortality at time w. It is linked to the survivor function as follows:

$$S(t) = e^{-H(t)} = e^{-\int_0^t h(w)dw} \tag{1}$$

where $H(t)$ is the cumulative hazard up to time t. It is assumed that $h(w) \geq 0$ and consequently, $H(t) \geq 0$. In the case of discrete time steps, the cumulative hazard can be re-expressed as $H(t) = \sum_{w=0}^{t} h(w)$ (Lawless, 2003, p. 11).

When mortality is observed through the remeasurements of permanent plots, the data are said to be interval censored (Lawless, 2003, p. 65). More specifically, it means that the exact time of death remains unknown. If the tree was initially alive at measurement t_1 but dead at measurement t_2, we know that $t_1 < T \leq t_2$. If the tree survived, then $T > t_2$. The probability that a tree survives over the interval given that it had already survived until the beginning of the interval is $S(t_2)/S(t_1)$. If we define the event E as the death of the tree, the probability that E occurs is simply the balance of probability:

$$\Pr(E \mid t_1, t_2) = 1 - \frac{S(t_2)}{S(t_1)} = 1 - \frac{e^{-H(t_2)}}{e^{-H(t_1)}} = 1 - e^{-\Delta H(t_1, t_2)} \tag{2}$$

where $\Delta H(t_1, t_2)$ is the difference in cumulative hazard, i.e. $\Delta H(t_1, t_2) = \sum_{w=t_1+1}^{t_2} h(w)$ in the context of discrete time steps. The hazard function $h(w)$ can be defined in many ways.

One of them is the proportional hazard model, also commonly referred to as the Cox model (Cox, 1972; Kalbfleisch and Schaubel, 2023), in which the hazard function is divided into two components:

$$h(w \mid \boldsymbol{x}) = h_0(w)e^{\boldsymbol{x\beta}} \tag{3}$$

where $h_0(w)$ is the baseline hazard at time w and $e^{\boldsymbol{x\beta}}$ is the proportional part of the model. This proportional part includes a row vector of explanatory variables ($\boldsymbol{x}$) and a column vector of parameters ($\boldsymbol{\beta}$). Using this proportional hazard, the difference in cumulative hazard becomes:

$$\Delta H(t_1, t_2) = e^{\boldsymbol{x\beta}} \sum_{w=t_1+1}^{t_2} h_0(w) \tag{4}$$

If we assume a constant hazard, i.e. $h_0(w) = e^{\alpha_0}$, the difference in cumulative hazard shown in Eq. 4 reduces to:

$$\Delta H(t_1, t_2) = e^{\boldsymbol{x\beta}+\alpha_0+\ln(\Delta t)} \tag{5}$$

where $\Delta t = t_2 - t_1$. The model shown in Eq. 2 with its difference in cumulative hazard as in Eq. 5 is a logistic model using a complementary log-log link function (McCullagh and Nelder, 1989, p. 31) and the offset variable $\ln(\Delta t)$. An offset is defined as a variable whose associated parameter is assumed to be equal to 1 (McCullagh and Nelder, 1989, p. 206). With the parameterization shown in Eq. 5, the offset variable $\ln(\Delta t)$ is equivalent to assuming that $e^{-e^{\boldsymbol{x\beta}+\alpha_0}}$ stands for the annual mortality rate, which remains constant over the interval $[t_1 + 1, t_2]$ (Fortin et al., 2008).

The constant hazard in Eq. 5 is a single parameter, but it could also be a function of average climate variables such that:

$$\Delta H(t_1, t_2) = e^{\boldsymbol{x\beta}+\bar{\boldsymbol{z}}\boldsymbol{\alpha}+\ln(\Delta t)} \tag{6}$$

where $\bar{\boldsymbol{z}}$ typically contains 30-year normals or interval-averaged climate variables, i.e. $\bar{\boldsymbol{z}} = \frac{\sum_{w=t_1+1}^{t_2} \boldsymbol{z}_w}{t_2 - t_1}$, and $\boldsymbol{z}_w = (1, z_{w,1}, z_{w,2}, \ldots)$ with the $z_{w,l}$ being the different climate variables measured at time w, and $\boldsymbol{\alpha}$ is a column vector of parameters, such that $\boldsymbol{\alpha} = (\alpha_0, \alpha_1, \alpha_2, \ldots)^{\mathrm{T}}$.

In contrast to Eq. 6, it can be assumed that the hazard is not constant, such that $h_0(w) = e^{\boldsymbol{z}_w \boldsymbol{\alpha}}$. Therefore, the difference in cumulative hazard shown in Eq. 4 can be re-expressed as:

$$\Delta H(t_1, t_2) = e^{\boldsymbol{x}\boldsymbol{\beta}} \sum_{w=t_1+1}^{t_2} e^{\boldsymbol{z}_w \boldsymbol{\alpha}} \tag{7}$$

Basically, the differences in cumulative hazard shown in Eqs 6 and 7 provide the framework to test whether an annual CSI leads to a better fit than an average CSI for the same vector of responses and the same explanatory variables in $\boldsymbol{x}$ and in the $\boldsymbol{z}$ vectors ($\boldsymbol{z}_w$ or $\bar{\boldsymbol{z}}$). These models can be fitted using the maximum likelihood method. In case of hierarchical structure, a random effect (u) can be added to the product $\boldsymbol{x}\boldsymbol{\beta}$ in both models under the assumption that $u \sim \mathcal{N}(0, \sigma_u^2)$. The NLMIXED procedure in SAS (SAS Institute Inc., 2023) allows for the fit of such models. A code sample can be found in Section S1 of the Supplementary Material.

Because the random effect does not enter linearly in the model, the predictions conditional on the mode of the random effect distribution are not population-averaged predictions (McCulloch et al., 2008, p. 190; Fortin, 2013; Melo et al., 2017). Considering the annual CSI shown in Eq. 7, population-averaged predictions are obtained through the integration of the conditional probabilities over the distribution of the random effect as follows:

$$\begin{aligned} \Pr(E \mid t_1, t_2) &= 1 - \mathbb{E}_u \left[e^{-e^{\boldsymbol{x}\boldsymbol{\beta}+u} \sum_{w=t_1+1}^{t_2} e^{\boldsymbol{z}_w \boldsymbol{\alpha}}} \right] \\ &= 1 - \int_{-\infty}^{\infty} e^{-e^{\boldsymbol{x}\boldsymbol{\beta}+u} \sum_{w=t_1+1}^{t_2} e^{\boldsymbol{z}_w \boldsymbol{\alpha}}} \mathrm{pdf}(u) du \end{aligned} \tag{8}$$

where $\mathrm{pdf}(u)$ is the density of u calculated from the normal distribution $\mathcal{N}(0, \sigma_u^2)$. Since σ_u^2 is unknown, it is replaced by its estimate. The integral shown in Eq. 8 has no closed form, but

it can be approximated using Gauss-Hermite quadrature (e.g., Pinheiro and Bates, 1995). The method is described in details in Fortin (2013). The same rationale applies to the mixed-effects version of the average CSI shown in Eq. 6.

2.2 Data

The data we used come from the Forest Growth and Yield program of the Ontario Ministry of Natural Resources (MNR), which aims at monitoring forest stand dynamics through a network of permanent plots in managed and unmanaged forests across the province (MNRF, 2023). This network includes two types of plots: permanent growth plot (PGP) and permanent sample plot (PSP). A PGP is a single growth plot of area ranging from 400 to 1000 m^2. In contrast, a PSP consists of a cluster of three 400-m^2 plots. Henceforth, terms "plot" and "cluster" will be used to refer to a single growth plot and a group of plots, respectively. In this context, a PGP is considered as a cluster of one plot. In these plots, all trees with diameter at breast height (DBH, measured at 1.3 m height) greater than or equal to 2.5 cm are tagged and measured.

The first measurements were taken in 1961 and the latest in 2022. We selected all the plots that had been measured at least twice. For each plot, the successive measurements were paired to create non overlapping intervals. The first measurement of each pair provided the initial conditions for each tree that was measured, whereas the second measurement confirmed whether these individuals had survived or died during the interval. These intervals based on individual tree remeasurements were the observations to which our mortality models were fitted.

The current inventory protocol specifies the tagging of trees as small as 2.5 cm in DBH. However, early versions of the protocol used different thresholds so that there was a great deal of missing observations for smaller trees. In contrast, the monitoring of merchantable trees, those with DBH $\geq$ 9.1 cm, was more reliable. Consequently, we used only merchantable trees in our analysis.

There was some variability in the interval duration which ranged from 1 to 29 years, with a median of 5 years. As trees grow and die, the initial conditions of an interval become less representative of the average conditions during that interval. For this reason, we discarded intervals that were longer than 10 years. We gathered these non overlapping intervals for eight commercial species in Ontario, which were among the most abundant ones in the original data: *Abies balsamea* Mill., *Acer saccharum* Marsh., *Betula papyrifera* Marsh., *Picea glauca* (Moench) Voss., *Picea mariana* BSP, *Pinus banksiana* Lamb., *Pinus strobus* L. and *Populus tremuloides* Michx. A summary of the dataset can be found in Table 1. The distribution of the plots with at least one merchantable tree of these species is shown in Figure 1.

(Insert Table 1 here)

(Insert Figure 1 here)

We retrieved the climate variables using the BioSIM application. BioSIM is a weather generator that spatially interpolates the meteorological time series at any geographical location from those observed in the nearest weather stations (Régnière et al., 1995, 2017). BioSIM is available as a Web API with an R client that facilitates the access to these interpolated meteorological time series as well as climate forecasts under different climate scenarios (Fortin et al., 2022).

More specifically, we used the Web API of BioSIM to retrieve the annual climate variables that were linked to our hypotheses H2, H3, and H4: mean temperature from June to August (°C), mean minimum January temperature (°C), total precipitation from March to May (mm), and total precipitation from June to August (mm). From these annual values, we also computed the average of each variable over the remeasurement intervals. These averages are the interval-averaged climate variables we referred to in the previous sections of this paper.

BioSIM can also provide normals of these variables for different 30-year periods: 1951-1980, 1961-1990, 1971-2000, 1981-2010, and 1991-2020. For each interval, we selected the 30-year period whose median was the closest to the median of the interval. For instance, the

1981-2010 normals would be retained for an interval covering the period 1993-1999, and so on. A summary of the 30-year normals observed in the dataset is shown in Table 2. To provide a better idea of the mean annual temperature and total annual precipitation in Ontario, the 30-year normals based on the 1981-2010 period are illustrated in Figure 2.

(Insert Table 2 here)

(Insert Figure 2 here)

For further information on the climate variables, the reader is referred to the Supplementary Material, which contains summaries of the interval-averaged climate variables (Section S2) and the annual climate variables (Section S3). The mean variances of the annual climate variables can also be found in Section S4.

2.3 Mortality modelling

We tested the general model (Eq. 2) with different parametrizations for the difference in cumulative hazard ($\Delta H(t_1, t_2)$). We first tested a null model ($\mathcal{M}_{\text{NUL}}$), that included a single parameter and no covariates:

$$\mathcal{M}_{\text{NUL}} : \Delta H(t_1, t_2) = e^{\alpha_0} \tag{9}$$

We then tested the constant-hazard model (Eq. 5) with plot and tree-level variables. After some preliminary trials, the following basic model ($\mathcal{M}_{\text{BAS}}$) was selected:

$$\mathcal{M}_{\text{BAS}} : \Delta H(t_1, t_2) = e^{\alpha_0 + \ln(\Delta t) + \beta_1 \text{DBH} + \beta_2 \text{DBH}^2 + \beta_3 \text{BAL} + \beta_4 \text{Harvest} + \beta_5 \text{DBH}\cdot\text{BAL}} \tag{10}$$

where BAL is the basal area of trees with DBH larger than that of the subject tree (m^2ha^{-1}), and Harvest is a dummy variable that accounts for the occurrence of harvesting during the interval. We kept a particular effect or interaction in the model only if its associated parameter was significantly different from 0 at a probability level of 0.05. The only exceptions

to this rule were parameters α_0 and β_1. Parameter α_0 was kept in the model whether it was significant or not because it stands for the basic hazard and we could not assume that this basic hazard was null. Likewise, parameter β_1 was kept in the model whether it was significant or not whenever β_2 was significantly different from 0 in accordance with the recommendation of Draper and Smith (1998, p. 266) on polynomial models.

As suggested in Fortin et al. (2019), we used average Pearson residuals to check whether the effects of the explanatory variables were properly taken into account in the model. The observations are split into groups that correspond to even classes of a particular explanatory variable. Then, the average Pearson residual for class k (r_k) of the explanatory variable can be calculated as:

$$r_k = \frac{p_k - \bar{\hat{\pi}}}{\sqrt{\bar{\hat{\pi}}(1-\bar{\hat{\pi}})/n_k}} \tag{11}$$

where p_k is the proportion of dead trees in the observations of class k, $\bar{\hat{\pi}}$ is the average of the model predictions, and n_k is the number of observations in class k. Under the assumption that the model is correct, the product $n_k p_k$ approximately follows a binomial distribution with mean $n_k\bar{\hat{\pi}}$. If n_k is large, then the distribution of p_k is approximately normal with mean $\bar{\hat{\pi}}$ and variance $\bar{\hat{\pi}}(1-\bar{\hat{\pi}})/n_k$, so that r_k approximately follows a standard normal distribution (McCullagh and Nelder, 1989, p. 104). When plotting average Pearson residuals against classes of a particular explanatory variable, it is expected that these residuals are close to 0 and do not exhibit any linear or quadratic patterns. With a little algebra, it can be shown that the sum $\sum_k r_k^2$ is equivalent to the Hosmer-Lemeshow goodness-of-fit statistics (Hosmer and Lemeshow, 2000, p. 148).

Given the hierarchical structure of the data, the existence of plot or cluster random effects could be reasonably assumed. The implementation of the models in the NLMIXED procedure (SAS Institute Inc., 2023) allows the specification of random effects. Consequently, we tested a mixed-effects model ($\mathcal{M}_{\text{MIX}}$) by adding a cluster random effect in the basic model ($\mathcal{M}_{\text{BAS}}$).

Building on this mixed-effects model, we alternately tested 30-year normals, interval-

averaged climate variables, and annual climate variables, leading to models $\mathcal{M}_{\text{NOR}}$, $\mathcal{M}_{\text{INT}}$, and $\mathcal{M}_{\text{ANN}}$, respectively. For each implementation, we tested the four climate variables: mean temperature from June to August, mean minimum January temperature, total precipitation from March to May, and total precipitation from June to August. In cases of persistent quadratic patterns in the average Pearson residuals, the squares of these variables were also tested in the models.

For each species, we compared the models through the well-known Bayesian Information Criterion (BIC) (Pinheiro and Bates, 2000, p. 83). The BIC is calculated from the model log-likelihood. Provided a set of candidate models fitted to the same vector of response variables, the model with the smallest BIC value is considered as being the most parsimonious one, that is the model exhibiting the best trade-off between model precision and simplicity.

There is no doubt that the BIC is helpful in selecting the most parsimonious model, but it may happen that the difference in BIC is not enough to clearly rule out some candidate models. Burnham and Anderson (2002, p. 302) used the BIC to determine the Bayesian posterior model probabilities under the assumption of equal prior model probabilities:

$$\Pr(\mathcal{M}_i) = \frac{e^{-\frac{1}{2}\Delta\text{BIC}_i}}{\sum_m e^{-\frac{1}{2}\Delta\text{BIC}_m}} \tag{12}$$

where ΔBIC_i and ΔBIC_m are the differences between the BIC of model $\mathcal{M}_i$ or $\mathcal{M}_m$ and the BIC of the "best" model. Note that there are five candidate models: $\mathcal{M}_{\text{NUL}}$, $\mathcal{M}_{\text{BAS}}$, $\mathcal{M}_{\text{NOR}}$, $\mathcal{M}_{\text{INT}}$, and $\mathcal{M}_{\text{ANN}}$. Consequently, the indices $i, m \in (1, 2, 3, 4, 5)$. A probability close to 1 for the "best" model indicates that the other candidate models can be ruled out. These Bayesian posterior probabilities were calculated for the candidate models of each species.

We also checked the goodness of fit of the candidate models using the area under the receiver operating characteristic (ROC) curve. The area under the ROC curve (AUC) has been widely used to evaluate a model's ability to discriminate positive and negative outcomes (Lasko et al., 2005). In the context of this study, a positive outcome means mortality, whereas survival can be interpreted as a negative outcome. Let us assume the existence of a cutpoint

c and classify all the observations with model predictions larger than c as positive outcomes. The sensitivity of a model is defined as the ratio of correctly classified positive outcomes to the observed number of positive outcomes. Likewise, model specificity is the correctly classified negative outcomes to the observed number of negative outcomes. Plotting model sensitivity against one minus the model specificity for the whole range $0 < c < 1$ yields the ROC curve. In other words, the ROC curve provides the sensitivity and specificity for all possible cutpoints. The AUC is simply the area under this curve. Hosmer and Lemeshow (2000) suggested the following rule of thumb: an AUC $= 0.5$ means no discrimination; $0.7 \leq$ AUC < 0.8 is considered acceptable discrimination; $0.8 \leq$ AUC < 0.9 is considered excellent discrimination and AUC ≥ 0.9 is considered outstanding discrimination. The authors did not make any statement regarding models with AUC values smaller than 0.7, but following their rule of thumb, we can consider them as having a poor discrimination capacity.

3 Results

BIC values, Bayesian posterior model probabilities, and AUC values of the different models are shown in Table 3. For all species, the specification of a cluster random effect greatly improved the model fit as indicated by the sharp decrease in BIC. Adding climate variables in addition to the cluster random effect allowed to further improve the fit of the models. For seven out of eight species, the most parsimonious model included cluster random effects and either 30-year normals ($\mathcal{M}_{\text{NOR}}$) or interval-averaged climate variables ($\mathcal{M}_{\text{INT}}$). *Picea mariana* was the only species for which the most parsimonious model included cluster random effects and annual climate variables ($\mathcal{M}_{\text{ANN}}$).

(Insert Table 3 here)

For six species, the Bayesian posterior probability of the most parsimonious model was close to 1 indicating that other candidate models were no valid alternatives (Table 3). For *Pi-*

nus strobus, the models based on either 30-year normals ($\mathcal{M}_{\text{NOR}}$) or annual climate variables ($\mathcal{M}_{\text{ANN}}$) could be considered as valid alternatives to the model based on interval-averaged climate variables ($\mathcal{M}_{\text{INT}}$). For *Populus tremuloides*, the model using annual climate variables had a Bayesian posterior probability of 0.23 and therefore, it could also be considered as an alternative to model based on interval-averaged climate variables.

Regarding the AUC values, only the most parsimonious models of *Acer saccharum*, *Picea glauca*, *Pinus banksiana*, and *Pinus strobus* showed an acceptable discrimination following Hosmer and Lemeshow's rule of thumb (i.e. $0.7 \leq \text{AUC} < 0.8$). The most parsimonious models of the other four species had AUC values between 0.63 and 0.68. For each species, the form of the most parsimonious model was:

for *Abies balsamea*,

$$\mathcal{M}_{\text{INT}} : \Delta H(t_1, t_2) = e^{\beta_1 \text{DBH} + \beta_3 \text{BAL} + \beta_4 \text{Harvest} + \beta_5 \text{DBH} \cdot \text{BAL} + u + \alpha_0 + \alpha_2 \text{T}_{\text{minJ}} + \alpha_3 \text{T}_{\text{minJ}}^2 + \ln(\Delta t)}$$

for *Acer saccharum*,

$$\mathcal{M}_{\text{NOR}} : \Delta H(t_1, t_2) = e^{\beta_1 \text{DBH} + \beta_2 \text{DBH}^2 + \beta_3 \text{BAL} + \beta_4 \text{Harvest} + \beta_5 \text{DBH} \cdot \text{BAL} + u + \alpha_0 + \alpha_1 \text{T}_{\text{JJA}} + \alpha_2 \text{T}_{\text{minJ}} + \ln(\Delta t)}$$

for *Betula papyrifera*,

$$\mathcal{M}_{\text{NOR}} : \Delta H(t_1, t_2) = e^{\beta_1 \text{DBH} + \beta_2 \text{DBH}^2 + \beta_3 \text{BAL} + \beta_4 \text{Harvest} + u + \alpha_0 + \alpha_2 \text{T}_{\text{minJ}} + \ln(\Delta t)}$$

for *Picea glauca*,

$$\mathcal{M}_{\text{NOR}} : \Delta H(t_1, t_2) = e^{\beta_1 \text{DBH} + \beta_3 \text{BAL} + \beta_4 \text{Harvest} + \beta_5 \text{DBH} \cdot \text{BAL} + u + \alpha_0 + \alpha_2 \text{T}_{\text{minJ}} + \ln(\Delta t)}$$

for *Picea mariana*,

$$\mathcal{M}_{\text{ANN}} : \Delta H(t_1, t_2) = e^{\beta_1 \text{DBH} + \beta_3 \text{BAL} + \beta_4 \text{Harvest} + \beta_5 \text{DBH} \cdot \text{BAL} + u \sum_{w=t_1+1}^{t_2} e^{\alpha_0 + \alpha_5 \text{P}_{\text{JJA},w}}}$$

for *Pinus banksiana*,

$$\mathcal{M}_{\text{NOR}} : \Delta H(t_1, t_2) = e^{\beta_1 \text{DBH} + \beta_3 \text{BAL} + \beta_5 \text{DBH} \cdot \text{BAL} + u + \alpha_0 + \alpha_5 \text{P}_{\text{JJA}} + \ln(\Delta t)}$$

for *Pinus strobus*,

$$\mathcal{M}_{\text{INT}} : \Delta H(t_1, t_2) = e^{\beta_1 \text{DBH} + \beta_2 \text{DBH}^2 + \beta_3 \text{BAL} + \beta_4 \text{Harvest} + u + \alpha_0 + \alpha_2 \text{T}_{\text{minJ}} + \ln(\Delta t)}$$

for *Populus tremuloides*,

$$\mathcal{M}_{\text{INT}} : \Delta H(t_1, t_2) = e^{\beta_1 \text{DBH} + \beta_2 \text{DBH}^2 + \beta_3 \text{BAL} + \beta_4 \text{Harvest} + \beta_5 \text{DBH} \cdot \text{BAL} + u + \alpha_0 + \alpha_1 \text{T}_{\text{JJA}} + \alpha_4 \text{P}_{\text{MAM}} + \ln(\Delta t)}$$

where T_{JJA} is the mean temperature from June to August (°C), T_{minJ} is the mean minimum

January temperature (°C), P_{MAM} is the total precipitation from March to May (mm), and P_{JJA} is the total precipitation from June to August (mm). In the models $\mathcal{M}_{NOR}$, $\mathcal{M}_{INT}$ and $\mathcal{M}_{ANN}$, these symbols stand for the 30-year normals, the interval-averaged and the annual values, respectively. The parameter estimates of these models can be found in Table 4. Graphs showing average Pearson residuals against classes of DBH, BAL, and the climate variables are available in Section S5 of the Supplementary Material (Figures S1-S8).

(Insert Table 4 here)

To illustrate the effects of the climate variables, population-averaged predictions of mortality probabilities were produced using Gauss-Hermite quadrature to account for the cluster random effect (Figure 3). Mean temperature from June to August was found to have a significant effect in the models of *Acer saccharum* and *Populus tremuloides*. However, the results were divergent: warmer temperatures for these months induced an increase in mortality occurrence for *Populus tremuloides*, but a decrease for *Acer saccharum* (Figure 3a). Mean minimum January temperature had a significant effect in the models of five species: *Abies balsamea*, *Acer saccharum*, *Betula papyrifera*, *Picea glauca*, and *Pinus strobus* (Figure 3b). Warmer temperatures resulted in an increase of mortality occurrence for all species, except for *Acer saccharum*. It was noteworthy that the effect of this climate variable had a quadratic pattern in the model of *Abies balsamea*, with -21°C being the optimal mean minimum January temperature for survival. As for the total precipitation from March to May and from June to August, it was found to have a significant effect in the models of *Picea mariana*, *Pinus banksiana*, and *Populus tremuloides* (Figure 3c,d). Greater precipitation resulted in an increase of mortality occurrence for all three species.

(Insert Figure 3 here)

The effects of DBH, basal area of larger trees, and harvest occurrence are illustrated in Figures 4 and 5. The effect of DBH differed across the species. *Abies balsamea*, *Picea glauca*,

Picea mariana, and *Pinus banksiana* showed an increase of mortality occurrence along with increasing DBH, whereas *Acer saccharum*, *Betula papyrifera*, *Pinus strobus*, and *Populus tremuloides* exhibited a quadratic pattern (Figure 4a). Increases in basal area of larger trees resulted in greater mortality occurrence for all species (Figure 4b). The harvesting of trees during the remeasurement interval also increased the occurrence of mortality for most species, except *Pinus banksiana* where this effect was non significant (Figure 5).

(Insert Figure 4 here)

(Insert Figure 5 here)

4 Discussion

In this study, we defined a framework based on lifetime analysis that makes it possible to account for climate variables at different temporal resolutions. Our approach relies on a proportional hazard model, which has already been used to model tree mortality (Yaussy et al., 2013; Hämäläinen et al., 2016; Neumann et al., 2017). The originality of our approach lies in the fact that we use predictors not only in the proportional part as in the regular Cox model, but also in the baseline hazard. Since the baseline hazard is computed on an annual basis, it is a natural entry point for an annual climate sensitivity implementation (CSI).

4.1 Is the annual climate sensitivity implementation better?

Building on this framework and Bayesian posterior model probabilities, we compared an annual CSI with two average CSIs for eight tree species in Ontario. Contrary to our hypothesis H1, the annual CSI only proved better for one species, *Picea mariana*, and could be considered as an alternative to the average CSI for two other species, *Pinus strobus* and *Populus tremuloides*. Among the other five species, the average CSI based on 30-year normals unequivocally provided the most parsimonious model for four of them. In summary, we

found little evidence that an annual CSI is superior to an average CSI, whether it relies on interval-averaged climate variables or 30-year normals. Nevertheless, our study shows that an annual CSI can be an alternative to an average CSI for some species.

There are three factors that can explain this result. Firstly, our data are interval censored: the exact time of death of an individual remains unknown, although we know for sure that death happens during the remeasurement interval. This loss of information is known to impact the statistical efficiency (Brooks, 1982; Turrero, 1989). There is no evidence that the loss of efficiency is greater for the annual CSI than for the average CSIs, but this cannot be ruled out and should be investigated.

Secondly, it is possible that the year to year variability in the climate variables was not large enough to justify the use of annual variables. In other words, the 30-year normals or interval-averaged climate variables might already account for the climate variability across the plots.

Thirdly, depending on the species, the decline phase leading to mortality can often last several years (Cailleret et al., 2017). For instance, an increased mortality was still observed three years after the 2003 extreme drought in France (Bréda and Badeau, 2008). The annual CSI in our framework does not consider climate effects that go beyond the current year. A high temperature for a given year will induce an increase of the hazard for that year, but will not affect the hazard of the following years.

Manso et al. (2013) used a lifetime analysis approach similar to ours in the modelling of seed germination. They managed to account for a temporal dependence in their daily hazard function so that the hazard of a particular day would be affected by the hazard of the previous day. We unsuccessfully tried to include this serial dependence in our framework. It could be that this serial dependence of the hazard did not exist in our data, or more likely, that extreme climate events leading to a long declining phase were scarce in our dataset. To the best of our knowledge, nothing like the 2003 extreme drought in France happened in Ontario over the time span of our dataset. Hember et al. (2017) reported several droughts

that occurred in North America between 1981 and 2012. Some of them hit Canada, but mainly in the Prairies and interior British Columbia (Bonsal et al., 2011). In Ontario, the only extreme droughts occurred in 1966 and 1988 (Gabriel and Kreutzwiser, 1993). We tested the impact of these droughts in our models using dummy variables, but we did not find any significant effects. The performance of the different CSIs might have been different if more extreme climate events had been observed in the data. This remains to be tested, but the framework is still valid for such a comparison.

4.2 The effects of climate variables on tree mortality

Overall, the inclusion of climate variables in the models improved their fit as shown by the drops in BIC for all the species (Table 3). However, larger drops in BIC were observed with the basic model ($\mathcal{M}_{\text{BAS}}$) and the mixed-effects model ($\mathcal{M}_{\text{MIX}}$). For all models benefiting from a CSI, the marginal contribution of climate variables to the model fit remained relatively small once competition, tree size, and cluster random effects had been accounted for in the model. Power et al. (2024) evaluated the contribution of different categories of variables in models of tree mortality in the neighbouring province of Quebec. For most species, they found that competition, tree size, and stand age had greater contributions to the model fit than climate variables.

Random effects stand for the joint effect of unobserved variables, such as drainage and soil texture (Gregoire, 1987). In our data, we had a few site descriptors, but in many cases, their values were missing. Keeping only the records for which we had observed values of these site descriptors would have left a depleted dataset. Power et al. (2024) showed that these site descriptors also have a limited contribution to the model fit. The joint effect of these descriptors can be considered as part of the cluster random effect in our models. The cluster random effects might also include some unaccounted for climate variables as well. Fortin et al. (2008) evidenced the presence of an interval random effect in a mortality model applied to northern hardwood species. Given that many plots were remeasured only once,

the interval effect might be confounded with the cluster random effect in our study.

Regarding our hypotheses on the effect of temperature, the higher mortality occurrence associated with warmer summer temperatures (H2) was corroborated in the model of *Populus tremuloides*, but refuted in the model of *Acer saccharum*. These contradictory results can be related to the species distributions. *Acer saccharum* is a species of the temperate forest zone and its distribution extends further south in the United States (Godman et al., 1990), indicating that it can tolerate warmer temperatures than those observed in our dataset. In contrast, *Populus tremuloides* is an emblematic species of the boreal forest zone and the province of Ontario covers a large part of its distribution (Perala, 1990). Sharma (2021) also found that the effects of climate variables on stand height varied depending on the locations.

Our hypothesis of lower mortality occurrence associated with warmer winter temperatures (H3) was refuted for four out of five species where the mean minimum January temperature was found significant. It rather appears that these warmer winter temperatures are detrimental to the survival of *Abies balsamea*, *Betula papyrifera*, *Picea glauca*, and *Pinus strobus*. In fact, our hypothesis H3 was only corroborated in the model of *Acer saccharum*.

Winter temperatures in North America are much lower than those in Europe (Seager et al., 2002). It can be hypothesized that the physiology of some tree species, especially boreal ones, requires cold winter temperatures. Contrary to the general hypothesis that warmer winters favour growth (Huang et al., 2010), Oboite and Comeau (2021) reported greater annual diameter growth associated with shorter frost-free periods for *Picea glauca*, *Pinus banksiana*, and *Pinus contorta* Dougl. ex. Loud. in western Canada. Likewise, Dymond et al. (2019) found cooler fall temperatures were linked to greater diameter growth for *Picea mariana* on peatland in Minnesota, USA. The physiological explanation behind this dependence to cold temperatures still needs to be developed.

Greater precipitation resulted in increased mortality rates for *Picea mariana*, *Pinus banksiana*, and *Populus tremuloides*. This result was contrary to our hypothesis H4. Hember et al. (2017) also reported contradictory results in the relationship between soil water content and

tree mortality in North America; large water contents would be detrimental to tree survival for some species, such as *Pinus banksiana* and *Pinus strobus*. Contradictory results of the same kind have also been highlighted in other studies (Lines et al., 2010; Dietze and Moorcroft, 2011; Yaussy et al., 2013; Cortini et al., 2017; Sánchez-Pinillos et al., 2022). Greater precipitation has already been found to be detrimental to diameter growth for some species such as white pine (Sharma, 2023).

No satisfactory explanation has been provided to explain the contradictory positive relationship between water availability and mortality. Yaussy et al. (2013) hypothesized that this positive relationship might be the result of an over-representation of younger trees in their data, those being less affected by water scarcity than older trees. We found no evidence in our data to support their hypothesis.

An interesting point raised by Cortini et al. (2017) is that pine species are more tolerant to drought and that the threshold beyond which they are really affected by water scarcity might not have been reached in the data. This is a plausible explanation. In that case, it could be hypothesized that the true relationship between water availability and mortality is U-shaped for some species as Lines et al. (2010) observed in the eastern United States. The average Pearson residuals of the three species for which precipitation was a significant predictor showed that this water scarcity threshold is smaller than 125 mm for the total precipitation from March to May and 200 mm for the total precipitation from June to August (see Figures S5, S6, and S8 in the Supplementary Material).

4.3 The potential impacts of climate change

Using the 1995-2014 reference period, the climate projections of the Intergovernmental Panel on Climate Change (IPCC) for the 2041-2060 period under the Shared Socioeconomic Pathway "Middle of the Road" show the following trends in the climate variables we used (SSP2-4.5, see Gutiérrez et al., 2021):

- +1.7°C in mean temperature from June to August;

- +2.1°C in mean minimum January temperature;
- +5.3% in total precipitation from March to May;
- +2.1% in total precipitation from June to August.

The impacts of climate change are often anticipated through a space-for-time assumption (Picket, 1989). It is assumed that future mortality occurrence in a particular location will be similar to current mortality occurrence in locations subjected to a warmer climate.

Our models suggest that mortality occurrence will increase for *Betula papyrifera*, *Picea glauca*, *Pinus strobus*, and *Populus tremuloides* due to increasing summer and winter temperature. In the case of *Abies balsamea*, the response will be location dependent: a decrease of mortality occurrence can be anticipated in locations with cold winter temperature whereas an increase of mortality occurrence should be expected in locations with warmer winter temperature. On the contrary, mortality occurrence should slightly decrease for *Acer saccharum*. The increase in total precipitation from March to May will induce an increase of mortality occurrence for *Populus tremuloides*. The increase in total precipitation from June to August should also cause a slight increase of mortality occurrence for *Picea mariana* and *Pinus banksiana*. It must be stressed that the space-for-time assumption underlying these predictions does not account for an eventual lag caused by genetic adaptation to new climatic conditions (Klesse et al., 2020).

In its latest assessment report, the IPCC also predicts a greater occurrence of extreme climate events in the future due to climate change (Seneviratne et al., 2021). We did not go as far as to make a formal comparison between the annual and average CSIs in the context of greater occurrence of extreme climate events. We anticipate that models based on an annual CSI will be more sensitive to these extreme events and could produce more realistic predictions. This issue deserves further investigation.

4.4 Other effects and limitations

The effect of DBH on mortality has been traditionally found to be U shaped (Lines et al., 2010; Fortin et al., 2014). Although our predictions do not cover the smallest and largest diameters (Fig. 4a), the addition of the squared DBH in the model ensured the predictions would tend to the expected U-shaped pattern. This was true for four species, but still the squared DBH did not have a significant effect in the models of *Abies balsamea*, *Picea glauca*, *Picea mariana*, and *Pinus banksiana* (Table 4). The trees of these latter species rarely reach large diameters. In our data, the 97.5th percentile of their DBH distributions was smaller than 33 cm for all four species (Figure 4a). The absence of large DBH in the dataset as well as the truncation below the merchantable size might explain why the U-shaped pattern was not observed for these four species.

Increasing competition, as measured through the basal area of larger trees (BAL), is known to increase mortality occurrence. Our results are in line with those of previous studies (Rathbun et al., 2010; Fortin et al., 2014; Manso et al., 2015). Interestingly, the occurrence of harvesting also resulted in large increases in mortality occurrence. In black spruce dominated stands in Ontario, Thorpe et al. (2008) found that residual trees experienced mortality rates 12.6 times higher in the first year after partial harvesting compared to pre-harvest rates. Likewise, Bladon et al. (2008) estimated mortality rates to be 2.5 to 4 times greater after retention cutting in Alberta.

Other variables related to tree crown, social position, and vigour have been identified as predictors of individual tree mortality occurrence (Monserud and Sterba, 1999; Dobbertin and Brang, 2001; Fortin et al., 2008; Rathbun et al., 2010). Guillemette et al. (2008) also linked the occurrence of defects, such as canker and wounds, with higher mortality rates. Unfortunately, these variables were either not available or had so many missing observations in our dataset that they could not be integrated into our models. Adding these variables in the models would likely improve their performance.

Our study does not consider insect outbreaks. We initially intended to account for these in

our models, but our data did not allow for it. For instance, a spruce budworm (*Choristoneura fumiferana* Clemens) outbreak occurred in Ontario during the 1970s and 1980s (Blais, 1983). The outbreak peaked in 1981 and then, declined until 1998 (Candau and Fleming, 2005). Defoliations were limited to a few sectors of northeastern Ontario until 2018. Since then, the defoliated area has increased into what could be considered as a new outbreak (J.-N. Candau, personal communication). *Abies balsamea* and *Picea glauca* are the host species that most suffer from these outbreaks (Boulanger and Arsenault, 2004). In our data, 99% of the remeasurement intervals of *Abies balsamea* and 92% of those of *Picea glauca* started after 1991. Moreover, the latest remeasurement intervals could include up to four years of severe defoliation, whereas the outbreak-induced mortality usually peaks after this period (Pothier and Mailly, 2006). Nevertheless, we tried to include dummy variables in the models of these two species to distinguish outbreak periods from endemic periods, but their effects were found to be non significant. Fortin and Langevin (2012) managed to account for spruce budworm outbreaks in the mortality component of their individual-based growth model in Quebec. The main difference with our dataset is that theirs had many more observations during outbreak periods.

5 Conclusions

Our framework based on a lifetime analysis approach makes it possible (i) to integrate annual climate variables in models of tree mortality even if the observations were recorded over multiple-year intervals, and (ii) to compare the model performance with similar models using an average CSI. It is particularly well adapted to permanent-plot data because the remeasurement intervals are usually irregular and the data are interval censored.

Using this framework, we modelled tree mortality for eight species in Ontario and showed that the hypothesis (H1) of the annual CSI outperforming the average CSI could not be corroborated. However, the annual CSI proved to be an alternative to the average CSI for

some species. Accounting for serial dependence in the hazard function could be an avenue of improvement to the annual CSI. We also hypothesize that the annual CSI might prove statistically superior when there is a greater year-to-year variability and more extreme climate events than what we observed in our data. This remains to be tested and our framework could prove useful for further comparisons. Because extreme climate events will likely be more frequent in the future, we recommend using the annual CSI when it can be considered as an alternative to the average CSI, that is when its Bayesian posterior probability is greater than 0.05.

Our results on the effects of climate variables were surprising in most cases. The hypotheses that (H2) warmer summer temperature is detrimental to survival, that (H3) warmer winter temperature favours tree survival, and that (H4) lower spring and summer precipitation leads to greater mortality rates could not be corroborated either. Digging in the literature, we found that these contradictory results are not uncommon. We conclude that the effects of climate on tree mortality interact with other factors such as species distribution and ecophysiology.

Acknowledgements

We thank the Ministry of Natural Resources of Ontario for providing the permanent-plot data. Special thanks are due to Jean-Noël Candau (Canadian Forest Service) for providing information on spruce budworm outbreaks in Ontario and two anonymous reviewers for their constructive comments.

Funding

This project was part of the Silva21 research program funded by the Natural Sciences and Engineering Research Council of Canada (NSERC) through its Alliance Grants Research Program (NSERC ALLRP 55626520).

Data Availability Statement

The data are subject to a sharing agreement with the Ministry of Natural Resources (MNR) of Ontario and cannot be freely shared unless a similar agreement is signed with MNR authorities.

Competing Interests

The authors declare there are no competing interests.

References

Bladon, K. D., Lieffers, V. J., Silins, U., Landhäusser, S. M., and Blenis, P. V. (2008). Elevated mortality of residual trees following structural retention harvesting in boreal mixedwoods. *The Forestry Chronicle*, 84(1):70–75.

Blais, J. R. (1983). Trends in the frequency, extent, and severity of spruce budworm outbreaks in eastern Canada. *Canadian Journal of Forest Research*, 13:539–547.

Bonsal, B. R., Wheaton, E. E., Chipanshi, A. C., Lin, C., Sauchyn, D. J., and Wen, L. (2011). Drought research in Canada: A review. *Atmosphere-Ocean*, 49(4):303–319.

Boulanger, Y. and Arsenault, D. (2004). Spruce budworm outbreaks in eastern Quebec over the last 450 years. *Canadian Journal of Forest Research*, 34:1035–1043.

Bréda, N. and Badeau, V. (2008). Forest tree responses to extreme drought and some biotic events: Towards a selection according to hazard tolerance? *External Geophysics, Climate and Environment*, 340:651–662.

Brooks, R. J. (1982). On the loss of information through censoring. *Biometrika*, 69(1):137–144.

621 Burnham, K. P. and Anderson, D. R. (2002). *Model selection and multimodel inference. A practical information-theoretical approach. Second edition.* Springer-Verlag, New York, USA.

624 Cailleret, M., Jansen, S., Robert, E. M. R., Desoto, L., Aakala, T., Antos, J. A., Beikircher, B., Bigler, C., Bugmann, H., Caccianiga, M., ada, V., Camarero, J. J., Cherubini, P., Cochard, H., Coyea, M. R., ufar, K., Das, A. J., Davi, H., Delzon, S., Dorman, M., Gea-Izquierdo, G., Gillner, S., Haavik, L. J., Hartmann, H., Here, A.-M., Hultine, K. R., Janda, P., Kane, J. M., Kharuk, V. I., Kitzberger, T., Klein, T., Kramer, K., Lens, F., Levanic, T., Linares Calderon, J. C., Lloret, F., Lobo-Do-Vale, R., Lombardi, F., Lpez Rodrguez, R., Mkinen, H., Mayr, S., Mszros, I., Metsaranta, J. M., Minunno, F., Oberhuber, W., Papadopoulos, A., Peltoniemi, M., Petritan, A. M., Rohner, B., Sangesa-Barreda, G., Sarris, D., Smith, J. M., Stan, A. B., Sterck, F., Stojanovi, D. B., Suarez, M. L., Svoboda, M., Tognetti, R., Torres-Ruiz, J. M., Trotsiuk, V., Villalba, R., Vodde, F., Westwood, A. R., Wyckoff, P. H., Zafirov, N., and Martnez-Vilalta, J. (2017). A synthesis of radial growth patterns preceding tree mortality. *Global Change Biology*, 23(4):1675–1690.

636 Candau, J.-N. and Fleming, R. A. (2005). Landscape-scale spatial distribution of spruce budworm defoliation in relation to bioclimatic conditions. *Canadian Journal of Forest Research*, 35:2218–2232.

639 Commission for Environmental Cooperation (2010). North American Atlas - Political Boundaries. GIS layers produced by Natural Resources Canada, Instituto Nacional de Estadstica y Geografa (Mexico), and the United States Geological Survey.

642 Cortini, F., Comeau, P. G., Strimbu, V. C., Hogg, E. H., and Bokalo, M. (2017). Survival functions for boreal species in northwestern North America. *Forest Ecology and Management*, 402:177–185.

645 Cox, D. R. (1972). Regression models and life-tables. *Journal of the Royal Statistical Society: Series B (Methodological)*, 34(2):187–202.

647 Crookston, N. L., Rehfeldt, G. E., Dixon, G. E., and Weiskittel, A. R. (2010). Addressing
648 climate change in the forest vegetation simulator to assess impacts on landscape forest
649 dynamics. *Forest Ecology and Management*, 260:1198–1211.

650 Dietze, M. C. and Moorcroft, P. R. (2011). Tree mortality in the eastern and central United
651 States: patterns and drivers. *Global Change Biology*, 17:3312–3326.

652 Dobbertin, M. and Brang, P. (2001). Crown defoliation improves tree mortality models.
653 *Forest Ecology and Management*, 141:271–284.

654 Draper, N. R. and Smith, H. (1998). *Applied Regression Analysis. Third Edition*. John Wiley
655 & Sons, Inc., New York, USA.

656 Dymond, S. F., D'Amato, A. W., Kolka, R. K., Bolstad, P. V., Sebestyen, S. D., Gill, K.,
657 and Curzon, M. T. (2019). Climatic controls on peatland black spruce growth in relation
658 to water table variation and precipitation. *Ecohydrology*, 12:e2137.

659 Fortin, M. (2013). Population-averaged predictions with generalized linear mixed-effects
660 models in forestry: an estimator based on Gauss-Hermite quadrature. *Canadian Journal*
661 *of Forest Research*, 43:129–138.

662 Fortin, M., Bédard, S., DeBlois, J., and Meunier, S. (2008). Predicting individual tree mor-
663 tality in northern hardwood stands under uneven-aged management in southern Québec,
664 Canada. *Annals of Forest Science*, 65:205.

665 Fortin, M. and Langevin, L. (2012). Stochastic or deterministic single-tree models: is there
666 any difference in growth predictions? *Annals of Forest Science*, 69(2):271–282.

667 Fortin, M., Lavoie, J.-F., Régnière, J., and Saint-Amant, R. (2022). A Web API for weather
668 generation and pest development simulation in North America. *Environmental Modelling*
669 *& Software*, 157:105476.

Fortin, M., Pichancourt, J.-B., Climaco de Melo, L., Colin, A., and Caurla, S. (2019). The effect of stumpage prices on large-area forest growth forecasts based on socio-ecological models. *Forestry*, 92:339–356.

Fortin, M., Power, H., Van Couwenberghe, R., and Eskelson, B. N. I. (2023). The effect of climate on the occurrence and abundance of tree recruitment in the province of quebec, canada. *Forestry*, 97:147–161.

Fortin, M., Tremblay, S., and Schneider, R. (2014). Evaluating a single tree-based growth model for even-aged stands against the maximum size-density relationship: Some insights from balsam fir stands in Quebec, Canada. *The Forestry Chronicle*, 90(4):503–515.

Gabriel, A. O. and Kreutzwiser, R. D. (1993). Drought hazard in Ontario: A review of impacts, 1960-1989, and management implications. *Canadian Water Resources Journal*, 18(2):117–132.

Godman, R. M., Yawney, H. W., and Tubbs, C. H. (1990). *Silvics of North America. Volume 2: Hardwoods*, chapter Sugar Maple. Agricultural Handbook 654. USDA Forest Service, Washington, DC.

Gregoire, T. G. (1987). Generalized error structure for forest yield models. *Forest Science*, 33:423–444.

Guillemette, F., Bédard, S., and Fortin, M. (2008). Evaluation of a tree classification system in relation to mortality risk in Québec northern hardwoods. *The Forestry Chronicle*, 84(6):886–899.

Gutiérrez, J. M., Jones, R. G., Narisma, G. T., Alves, L. M., Amjad, M., Gorodetskaya, I. V., Grose, M., Klutse, N. A. B., Krakovska, S., Li, J., Martínez-Castro, D., Mearns, L. O., Mernild, S. H., Ngo-Duc, T., van den Hurk, B., and Yoon, J.-H. (2021). *Climate Change 2021: The Physical Science Basis. Contribution of Working Group I to*

694 *the Sixth Assessment Report of the Intergovernmental Panel on Climate Change*, chap-
695 ter Atlas. Cambridge University Press. Interactive Atlas available from Available from
696 http://interactive-atlas.ipcc.ch/. Consulted on February 18th, 2024.

697 Hämäläinen, A., Hujo, M., Heikkala, O., Junninen, K., and Kouki, J. (2016). Retention tree
698 characteristics have major influence on the post-harvest tree mortality and availability of
699 coarse woody debris in clear-cut areas. *Forest Ecology and Management*, 369:66–73.

700 Hartmann, H., Bastos, A., Das, A. J., Esquivel-Muelbert, A., Hammond, W. M., Martínez-
701 Vilalta, J., McDowell, N. G., Powers, J. S., Pugh, T. A. M., Ruthrof, K. X., and Allen,
702 C. D. (2022). Climate change risks to global forest health: Emergence of unexpected events
703 of elevated tree mortality worldwide. *Annual Review of Plant Biology*, 73:673–702.

704 Hember, R. A., Kurz, W. A., and Coops, N. C. (2017). Relationships between individual-tree
705 mortality and water-balance variables indicate positive trends in water stress-induced tree
706 mortality across north america. *Global Change Biology*, 23:1691–1710.

707 Hosmer, D. J. and Lemeshow, S. (2000). *Applied logistic regression*. John Wiley & Sons,
708 New York, 2nd edition.

709 Huang, J., Tardif, J. C., Bergeron, Y., Denneler, B., Berninger, F., and Girardin, M. P.
710 (2010). Radial growth response of four dominant boreal tree species to climate along a
711 latitudinal gradient in the easter Canadian boreal forest. *Global Change Biology*, 16:711–
712 731.

713 Kalbfleisch, J. D. and Schaubel, D. E. (2023). Fifty years of the Cox model. *Annual Review*
714 *of Statistics and Its Application*, 10:1–23.

715 Klesse, S., DeRose, R. J., Babst, F., Black, B. A., Anderegg, L. D. L., Axelson, J., Et-
716 tinger, A., Griesbauer, H., Guiterman, C. H., Harley, G., Harvey, J. E., Lo, Y.-H., Lynch,
717 A. M., OConnor, C., Restaino, C., Sauchyn, D., Shaw, J. D., Smith, D. J., Wood, L.,

718 Villanueva-Diaz, J., and Evans, M. E. K. (2020). Continental-scale tree-ring-based projec-
719 tion of Douglas-fir growth: Testing the limits of space-for-time substitution. *Global Change*
720 *Biology*, 26:5146–5163.

721 Larocque, G. R., Archambault, L., and Delisle, C. (2011). Development of the gap model
722 ZELIG-CFS to predict the dynamics of North American mixed forest types with complex
723 structures. *Ecological Modelling*, 222:2570–2583.

724 Lasko, T. A., Bhagwat, J. G., Zou, K. H., and Ohno-Machado, L. (2005). The use of
725 receiver operating characteristic curves in biomedical informatics. *Journal of Biomedical*
726 *Informatics*, 38:404–415.

727 Lawless, J. (2003). *Statistical models and methods for lifetime data*. John Wiley & Sons.

728 Li, R., Weiskittel, A. R., and Kershaw, Jr., J. A. (2011). Modeling annualized occurrence,
729 frequency, and composition of ingrowth using mixed-effects zero-inflated models and per-
730 manent plots in the acadian Forest Region of North America. *Canadian Journal of Forest*
731 *Research*, 41:2077–2089.

732 Lines, E. R., Coomes, D. A., and Purves, D. W. (2010). Influences of forest structure, climate
733 and species composition on tree mortality across the eastern US. *PLoS ONE*, 5(10):e13212.

734 Manso, R., Fortin, M., Calama, R., and Pardos, M. (2013). Modelling seed germination in
735 forest tree species through survival analysis. The *Pinus pinea* L. case study. *Forest Ecology*
736 *and Management*, 289:515–524.

737 Manso, R., Morneau, F., Ningre, F., and Fortin, M. (2015). Incorporating stochasticity
738 from extreme climatic events and multi-species competition relationships into single-tree
739 mortality models. *Forest Ecology and Management*, 354:243–253.

740 Maringer, J., Stelzer, A.-S., Paul, C., and Albrecht, A. T. (2021). Ninety-five years of observed
741 disturbance-based tree mortality modeled with climate-sensitive accelerated failure time
742 models. *European Journal of Forest Research*, 140:255–272.

743 McCullagh, P. and Nelder, J. A. (1989). *Generalized linear models*. Chapman & Hall/CRC,
744 New York, USA.

745 McCulloch, C., Searle, S., and Neuhaus, J. M. (2008). *Generalized, linear, and mixed models*.
746 John Wiley & Sons, New York.

747 Melo, L. C., Schneider, R., Manso, R., Saucier, J.-P., and Fortin, M. (2017). Using survival
748 analysis to predict the harvesting of forest stands in Quebec, Canada. *Canadian Journal*
749 *of Forest Research*, 47:1066–1074.

750 Metsaranta, J., Fortin, M., White, J. C., Sattler, D., Kurz, W. A., Penner, M., Edwards, J.,
751 Hays-Byl, W., Comeau, R., and Roy, V. (2024). Climate sensitive growth and yield models
752 in canadian forestry: Challenges and opportunities. *The Forestry Chronicle*, Submitted.

753 MNRF (2023). Ontario growth and yield Program PSP and PGP reference manual. Science
754 and Research Technical Manual, Ontario Ministry of Natural Resources and Forestry,
755 Science and Research Branch, Peterborough, ON.

756 Monserud, R. A. and Sterba, H. (1999). Modeling individual tree mortality for Austrian
757 forest species. *Forest Ecology and Management*, 113:109–123.

758 Neumann, M., Mues, V., Moreno, A., Hasenauer, H., and Seidl, R. (2017). Climate variability
759 drives recent tree mortality in europe. *Global Change Biology*, 23:4788–4797.

760 Oboite, F. O. and Comeau, P. G. (2021). Climate sensitive growth models for predicting
761 diameter growth of western Canadian boreal tree species. *Forestry*, 94:363–373.

762 Perala, D. A. (1990). *Silvics of North America. Volume 2: Hardwoods*, chapter Quaking
763 Aspen. Agricultural Handbook 654. USDA Forest Service, Washington, DC.

764 Picket, S. T. A. (1989). *Long-Term Studies in Ecology. Approaches and Alternatives*, chapter
765 Space-for-time substitution as an alternative to long-term studies, pages 110–135. Springer-
766 Verlag, New York, USA.

767 Pinheiro, J. C. and Bates, D. M. (1995). Approximations to the log-likelihood function in
768 the nonlinear mixed-effects model. *Journal of Computational and Graphical Statistics*,
769 4(1):12–35.

770 Pinheiro, J. C. and Bates, D. M. (2000). *Mixed-effects models in S and S-PLUS*. Springer-
771 Verlag, New York, USA.

772 Pothier, D. and Mailly, D. (2006). Stand-level prediction of balsam fir mortality in relation
773 to spruce budworm defoliation. *Canadian Journal of Forest Research*, 36:1631–1640.

774 Power, H., Auger, I., Lambert, M.-C., Fortin, M., and Bouchard, M. (2024). Modeling
775 background mortality for nine tree species of canada's boreal forest: how ontogeny, com-
776 petition, site characteristics and climate influence the phenomenon. *Canadian Journal of*
777 *Forest Research*, page In press.

778 Pretzsch, H., Biber, P., and Ďurský (2002). The single tree-based stand simulator SILVA:
779 construction, application and evaluation. *Forest Ecology and Management*, 162:3–21.

780 Rathbun, L. C., LeMay, V., and Smith, N. (2010). Modeling mortality in mixed-species
781 stands of coastal British Columbia. *Canadian Journal of Forest Research*, 40:1517–1528.

782 Régnière, J., Cooke, B., and Bergeron, V. (1995). BioSIM: A computer-based decision support
783 tool for seasonal planning of pest management activities. Information report lau-x-116,
784 Natural Resources Canada, Canadian Forest Service, Laurentian Forestry Centre.

785 Régnière, J., Saint-Amant, R., Béchard, A., and Moutaoufik, A. (2017). BioSIM 11 – User's
786 manual. Update of Information Report LAU-X-137, Natural Resources Canada, Canadian
787 Forest Service, Laurentian Forestry Centre.

788 Rose, Jr, C. E., Hall, D. B., Shiver, B. D., Clutter, M. L., and Borders, B. (2006). A multilevel
789 approach to individual tree survival prediction. *Forest Science*, 52(1):31–43.

790 Sánchez-Pinillos, M., D'Orangeville, L., Boulanger, Y., Comeau, P., Wang, J., Taylor, A. R.,
791 and Kneeshaw, D. (2022). Sequential droughts: A silent trigger of boreal forest mortality.
792 *Global Change Biology*, 28:542–556.

793 SAS Institute Inc. (2023). *SAS/STAT 15.3 User's Guide*, chapter The NLMIXED Procedure.
794 SAS Institute Inc., North Carolina, USA.

795 Seager, R., Battisti, D. S., Yin, J., Gordon, N., Naik, N., Clement, A. C., and Cane, M. A.
796 (2002). Is the Gulf Stream responsible for Europe's mild winters? *Quarterly Journal of*
797 *the Royal Meteorological Society*, 128(586):2563–2586.

798 Seneviratne, S. I., Zhang, X., Adnan, M., Badi, W., Dereczynski, Di Luca, A., Ghosh, S.,
799 Iskandar, I., Kossin, J., Lewis, S., Otto, F., Pinto, I., Satoh, M., Vicente-Serrano, S. M.,
800 Wehner, M., and Zhou, B. (2021). *Climate Change 2021: The Physical Science Basis.*
801 *Contribution of Working Group I to the Sixth Assessment Report of the Intergovernmental*
802 *Panel on Climate Change*, chapter Weather and Climate Extreme Events in a Changing
803 Climate, pages 1513–1766. Cambridge University Press, Cambridge, United Kingdom.

804 Sharma, M. (2021). Climate effects on jack pine and black spruce productivity in natu-
805 ral origin mixed stands and site index conversion equations. *Trees, Forests and People*,
806 6:100089.

807 Sharma, M. (2023). Climate-sensitive diameter growth models for white spruce and white
808 pine plantations. *Forests*, 14:2457.

809 Thorpe, H. C., Thomas, S. C., and Caspersen, J. P. (2008). Tree mortality following partial
810 harvests is determined by skidding proximity. *Ecological Applications*, 18(7):1652–1663.

811 Turrero, A. (1989). On the relative efficiency of grouped and censored survival data.
812 *Biometrika*, 76(1):125–131.

813 Vanclay, J. K. (1994). *Modelling Forest Growth and Yield – Applications to Mixed Tropical*
814 *Forests*. CAB International, Wallingford, United Kingdom.

815 Yaussy, D. A., Iverson, L. R., and Matthews, S. N. (2013). Competition and climate affects
816 US hardwood-forest tree mortality. *Forest Science*, 59(4):416–430.

Tables

Table 1: Mean characteristics of the intervals for each species. Minimum and maximum values appear in parentheses. For all species, the minimum and maximum values of interval duration were 1 and 10 years, respectively. DBH: diameter at breast height. BAL: basal area of larger trees. Mortality occurrence is represented at the tree level. Harvesting occurrence is defined as one or more trees being harvested in the plot during the remeasurement interval.

	Abies balsamea	*Acer saccharum*	*Betula papyrifera*	*Picea glauca*	*Picea mariana*	*Pinus banksiana*	*Pinus strobus*	*Populus tremuloides*
Number of intervals	16804	71468	16336	15295	67959	84304	6239	26492
Mortality occurrence	10.6%	5.5%	9.7%	4.8%	8.0%	7.4%	7.9%	12.4%
Interval duration (yrs)	5.6	5.1	5.8	5.9	5.9	6.1	6.0	5.8
DBH (cm)	13.7 (9.1,42.7)	21.1 (9.1,91.0)	15.0 (9.1,55.0)	15.6 (9.1,66.0)	13.6 (9.1,41.9)	14.3 (9.1,51.3)	24.2 (9.1,90.2)	17.0 (9.1,65.4)
BAL (m^2ha^{-1})	20.2 (0.0,73.4)	17.5 (0.0,73.1)	17.9 (0.0,71.8)	15.8 (0.0,76.6)	17.0 (0.0,76.0)	12.2 (0.0,51.0)	21.5 (0.0,63.9)	15.1 (0.0,55.9)
Basal area (m^2ha^{-1})	28.3 (0.3,77.1)	25.2 (1.7,81.2)	25.8 (0.9,77.1)	26.9 (0.3,77.1)	27.7 (0.3,77.1)	23.6 (0.2,57.6)	35.0 (1.7,68.4)	27.3 (0.3,79.0)
Stem density (trees ha^{-1})	1531 (25,3853)	738 (50,2525)	1324 (25,3853)	1611 (50,3753)	1904 (50,4203)	1754 (25,4203)	1042 (25,3277)	1594 (25,3978)
Harvest occurrence	2.4%	18.1%	1.3%	2.4%	1.4%	1.0%	12.2%	1.0%

Table 2: Mean of 30-year normals for each species as observed in the dataset. Minimum and maximum values appear in parentheses.

Climate variable	*Abies balsamea*	*Acer saccharum*	*Betula papyrifera*	*Picea glauca*	*Picea mariana*	*Pinus banksiana*	*Pinus strobus*	*Populus tremuloides*
Mean annual temperature (°C)	2.2 (-0.1,6.7)	5.6 (2.6,9.7)	2.6 (-0.1,8.3)	2.1 (-0.1,7.7)	2.0 (-0.5,5.4)	2.3 (-0.5,5.0)	5.7 (1.1,9.4)	2.3 (-0.5,6.9)
Mean temperature from June to August (°C)	16.4 (13.9,19.3)	18.0 (15.4,21.4)	16.5 (13.9,20.0)	16.2 (13.9,19.6)	16.3 (13.9,18.4)	16.6 (14.2,18.4)	18.2 (14.7,21.0)	16.5 (13.9,19.5)
Mean minimum January temperature (°C)	-21.7 (-26.7,-12.0)	-14.5 (-21.4,-6.6)	-20.6 (-25.3,-9.1)	-21.6 (-26.7,-8.5)	-21.9 (-26.7,-14.9)	-21.4 (-26.0,-15.0)	-14.5 (-24.5,-6.6)	-21.2 (-27.4,-10.4)
Total annual precipitation (mm)	824 (645,1191)	1007 (785,1408)	812 (574,1213)	807 (654,1187)	771 (574,1150)	788 (574,1030)	997 (657,1202)	774 (574,1162)
Total precipitation from March to May (mm)	176 (121,255)	221 (178,330)	175 (115,252)	171 (123,252)	162 (115,252)	168 (115,221)	221 (137,259)	165 (115,253)
Total precipitation from June to August (mm)	261 (218,313)	257 (210,328)	259 (218,313)	255 (218,312)	264 (214,313)	267 (213,313)	257 (216,312)	266 (218,313)

Table 3: Bayesian information criterion (BIC) values, Bayesian posterior model probabilities and areas under the receiver operating characteristic curve (AUC) of the different models. $\mathcal{M}_{\text{NUL}}$: null model; $\mathcal{M}_{\text{BAS}}$: basic model; $\mathcal{M}_{\text{MIX}}$: model with cluster random effects; $\mathcal{M}_{\text{NOR}}$: model $\mathcal{M}_{\text{MIX}}$ with 30-year normals; $\mathcal{M}_{\text{INT}}$: model $\mathcal{M}_{\text{MIX}}$ with interval-averaged climate variables; $\mathcal{M}_{\text{ANN}}$: model $\mathcal{M}_{\text{MIX}}$ with annual climate variables. Values in bold font are those of the most parsimonious model for each species. ΔBIC: difference in BIC with the most parsimonious model. The ** symbol denotes a probability lower than 0.005.

Species	Model	BIC	ΔBIC	Posterior probability	AUC	Species	Model	BIC	ΔBIC	Posterior probability	AUC
Abies balsamea	$\mathcal{M}_{\text{NUL}}$	11341	1480	**	0.50	*Picea mariana*	$\mathcal{M}_{\text{NUL}}$	37839	5616	**	0.50
	$\mathcal{M}_{\text{BAS}}$	11253	1392	**	0.57		$\mathcal{M}_{\text{BAS}}$	36174	3951	**	0.66
	$\mathcal{M}_{\text{MIX}}$	9938	78	**	0.56		$\mathcal{M}_{\text{MIX}}$	32283	60	**	0.66
	$\mathcal{M}_{\text{NOR}}$	9918	57	**	0.59		$\mathcal{M}_{\text{NOR}}$	32248	24	**	0.69
	$\boldsymbol{\mathcal{M}_{\text{INT}}}$	**9861**	**0**	**1.00**	**0.65**		$\mathcal{M}_{\text{INT}}$	32242	19	**	0.68
	$\mathcal{M}_{\text{ANN}}$	9895	35	**	0.60		$\boldsymbol{\mathcal{M}_{\text{ANN}}}$	**32223**	**0**	**1.00**	**0.68**
Acer saccharum	$\mathcal{M}_{\text{NUL}}$	30637	2757	**	0.50	*Pinus banksiana*	$\mathcal{M}_{\text{NUL}}$	44584	9431	**	0.50
	$\mathcal{M}_{\text{BAS}}$	28973	1093	**	0.69		$\mathcal{M}_{\text{BAS}}$	38625	3471	**	0.77
	$\mathcal{M}_{\text{MIX}}$	27948	68	**	0.69		$\mathcal{M}_{\text{MIX}}$	35191	38	**	0.76
	$\boldsymbol{\mathcal{M}_{\text{NOR}}}$	**27880**	**0**	**1.00**	**0.70**		$\boldsymbol{\mathcal{M}_{\text{NOR}}}$	**35154**	**0**	**1.00**	**0.77**
	$\mathcal{M}_{\text{INT}}$	27910	30	**	0.70		$\mathcal{M}_{\text{INT}}$	35181	28	**	0.76
	$\mathcal{M}_{\text{ANN}}$	27907	27	**	0.70		$\mathcal{M}_{\text{ANN}}$	35173	20	**	0.77
Betula papyrifera	$\mathcal{M}_{\text{NUL}}$	10393	1231	**	0.50	*Pinus strobus*	$\mathcal{M}_{\text{NUL}}$	3462	393	**	0.50
	$\mathcal{M}_{\text{BAS}}$	10249	1087	**	0.59		$\mathcal{M}_{\text{BAS}}$	3178	109	**	0.72
	$\mathcal{M}_{\text{MIX}}$	9245	83	**	0.59		$\mathcal{M}_{\text{MIX}}$	3072	2	0.10	0.72
	$\boldsymbol{\mathcal{M}_{\text{NOR}}}$	**9162**	**0**	**1.00**	**0.63**		$\mathcal{M}_{\text{NOR}}$	3069	0	0.30	0.73
	$\mathcal{M}_{\text{INT}}$	9187	25	**	0.61		$\boldsymbol{\mathcal{M}_{\text{INT}}}$	**3069**	**0**	**0.32**	**0.73**
	$\mathcal{M}_{\text{ANN}}$	9176	14	**	0.61		$\mathcal{M}_{\text{ANN}}$	3070	0	0.29	0.73
Picea glauca	$\mathcal{M}_{\text{NUL}}$	5912	1000	**	0.50	*Populus tremuloides*	$\mathcal{M}_{\text{NUL}}$	19905	3203	**	0.50
	$\mathcal{M}_{\text{BAS}}$	5366	454	**	0.74		$\mathcal{M}_{\text{BAS}}$	18662	1961	**	0.68
	$\mathcal{M}_{\text{MIX}}$	4951	39	**	0.74		$\mathcal{M}_{\text{MIX}}$	16803	102	**	0.67
	$\boldsymbol{\mathcal{M}_{\text{NOR}}}$	**4912**	**0**	**1.00**	**0.76**		$\mathcal{M}_{\text{NOR}}$	16734	33	**	0.67
	$\mathcal{M}_{\text{INT}}$	4940	28	**	0.74		$\boldsymbol{\mathcal{M}_{\text{INT}}}$	**16701**	**0**	**0.77**	**0.68**
	$\mathcal{M}_{\text{ANN}}$	4944	32	**	0.74		$\mathcal{M}_{\text{ANN}}$	16704	2	0.23	0.68

Table 4: Parameter estimates of the most parsimonious models. The standard error appears in parentheses. n/a: not applicable. T_{JJA}: Mean temperature from June to August; T_{minJ}: Mean minimum January temperature; P_{MAM}: Total precipitation from March to May; P_{JJA}: Total precipitation from June to August.

Parameter and effect	Species and model							
	Abies balsamea $\mathcal{M}_{INT}$	*Acer saccharum* $\mathcal{M}_{NOR}$	*Betula papyrifera* $\mathcal{M}_{NOR}$	*Picea glauca* $\mathcal{M}_{NOR}$	*Picea mariana* $\mathcal{M}_{ANN}$	*Pinus banksiana* $\mathcal{M}_{NOR}$	*Pinus strobus* $\mathcal{M}_{INT}$	*Populus tremuloides* $\mathcal{M}_{INT}$
β_1 (DBH)	0.102 (0.011)	-8.36×10^{-2} (0.93×10^{-2})	-0.102 (0.021)	8.68×10^{-2} (0.88×10^{-2})	0.118 (0.006)	9.99×10^{-2} (0.55×10^{-2})	-0.140 (0.018)	-1.49×10^{-2} (1.93×10^{-2})
β_2 (DBH^2)	n/a	1.52×10^{-3} (0.11×10^{-3})	2.24×10^{-3} (0.47×10^{-3})	n/a	n/a	n/a	1.60×10^{-3} (0.27×10^{-3})	1.05×10^{-3} (0.31×10^{-3})
β_3 (BAL)	7.33×10^{-2} (0.83×10^{-2})	8.03×10^{-2} (0.53×10^{-2})	2.48×10^{-2} (0.44×10^{-2})	0.147 (0.009)	0.113 (0.005)	0.223 (0.005)	3.46×10^{-2} (0.60×10^{-2})	0.136 (0.008)
β_4 (Harvest)	0.728 (0.160)	0.485 (0.051)	0.767 (0.223)	0.825 (0.238)	1.34 (0.117)	n/a	0.824 (0.162)	0.702 (0.243)
β_5 (DBH×BAL)	-3.079×10^{-3} (0.53×10^{-3})	-2.13×10^{-3} (0.25×10^{-3})	n/a	-5.22×10^{-3} (0.54×10^{-3})	-4.39×10^{-3} (0.34×10^{-3})	-7.84×10^{-3} (0.32×10^{-3})	n/a	-2.87×10^{-3} (0.38×10^{-3})
α_0	10.29 (1.66)	-2.86 (0.97)	-8.74×10^{-2} (49.88×10^{-2})	-4.48 (0.60)	-9.14 (0.22)	-11.11 (0.48)	-2.44 (0.57)	-15.01 (1.13)
α_1 (T_{JJA})	n/a	-0.144 (0.043)	n/a	n/a	n/a	n/a	n/a	0.350 (0.060)
α_2 (T_{minJ})	1.64 (0.16)	-4.48×10^{-2} (1.44×10^{-2})	0.198 (0.021)	0.178 (0.026)	n/a	n/a	7.01×10^{-2} (2.55×10^{-2})	n/a
α_3 (T^2_{minJ})	3.94×10^{-2} (0.40×10^{-2})	n/a	n/a	n/a	n/a	n/a	n/a	n/a
α_4 (P_{MAM})	n/a	n/a	n/a	n/a	n/a	n/a	n/a	1.82×10^{-2} (0.20×10^{-2})
α_5 (P_{JJA})	n/a	n/a	n/a	n/a	$6.06 \times^{-3}$ ($0.62 \times^{-3}$)	1.23×10^{-2} (0.17×10^{-2})	n/a	n/a
σ^2_u	1.32 (0.13)	0.580 (0.044)	1.52 (0.15)	1.57 (0.21)	1.24 (0.08)	1.03 (0.07)	0.569 (0.163)	1.90 (0.15)

Figures

Figure 1: Distribution of the permanent plots of the Ontario Growth and Yield program with at least one merchantable tree of the selected species. The province of Ontario is delineated in yellow. These maps were created using QGIS version 3.28 and assembled from the following data sources: boundaries from the North American Atlas (Commission for Environmental Cooperation, 2010), plot locations from the database of the Forest Growth and Yield program of the Ontario Ministry of Natural Resources.

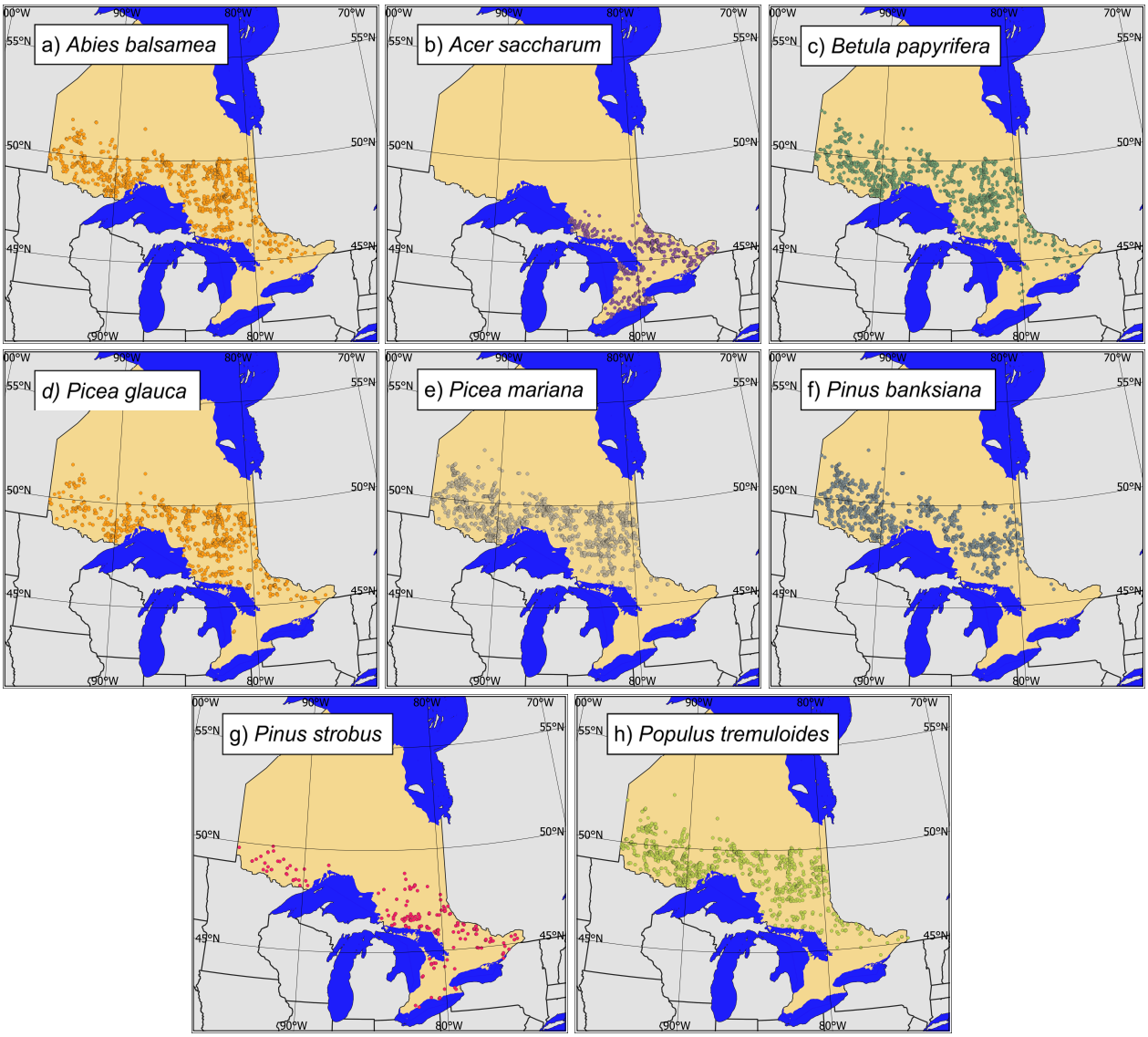

Figure 2: Mean annual temperature (a) and total annual precipitation (b) in Ontario for the 1981-2010 period. These maps were created using QGIS version 3.28 and assembled from the following data sources: boundaries from the North American Atlas (Commission for Environmental Cooperation, 2010), climate data from the BioSIM application (Régnière et al., 1995, 2017; Fortin et al., 2022).

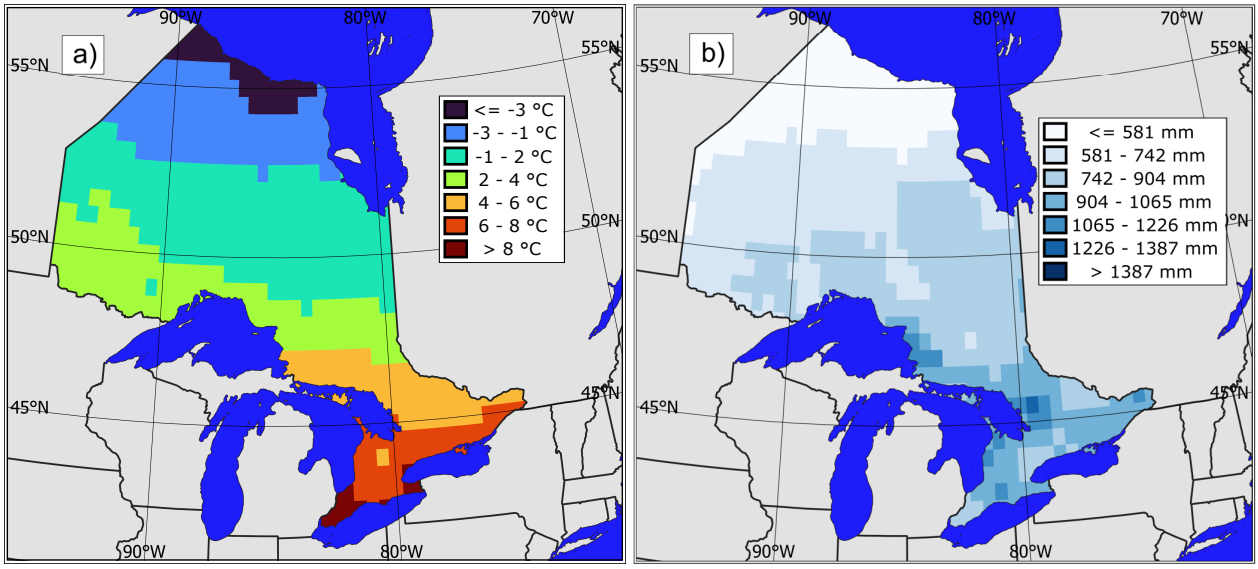

Figure 3: Predicted five-year probability of mortality in function of climate variables. It was assumed there was no harvesting during the interval (Harvest = 0). Other variables were set to their means as shown in Tables 1 and 2. For *Picea mariana*, the annual climate variables were generated under the assumption of normal distribution with mean and variance as observed in the dataset (see Sections S3 and S4 of the Supplementary Material). The range of the climate variables was delimited by the 2.5th and 97.5th percentiles of the distribution observed in the dataset.

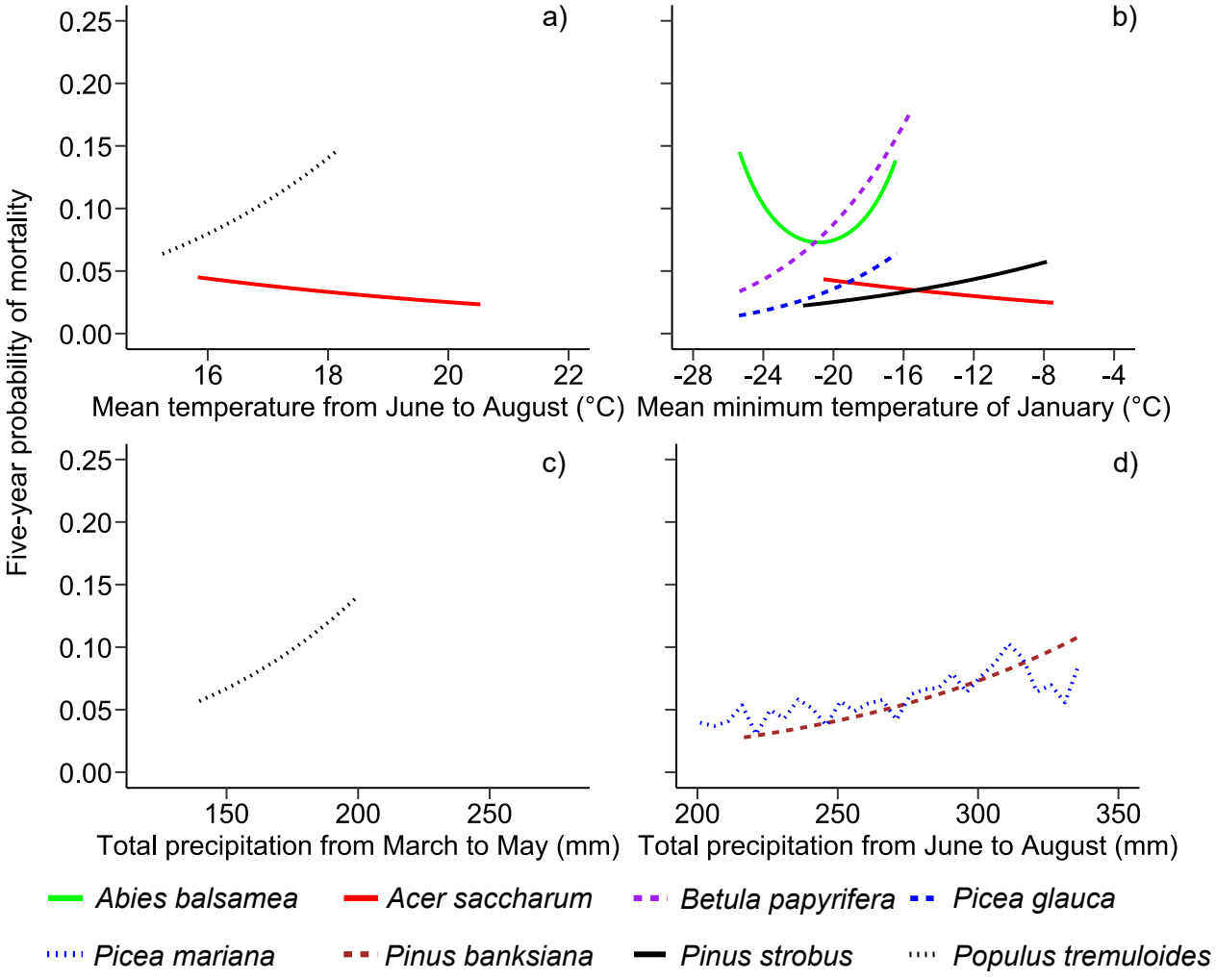

Figure 4: Predicted five-year probability of mortality in function of DBH (a) and basal area of larger trees (b). It was assumed there was no harvesting during the interval (Harvest = 0). Other variables were set to their means as shown in Tables 1 and 2. The range of DBH and basal area of larger trees was delimited by the 2.5th and 97.5th percentiles of the distribution observed in the dataset.

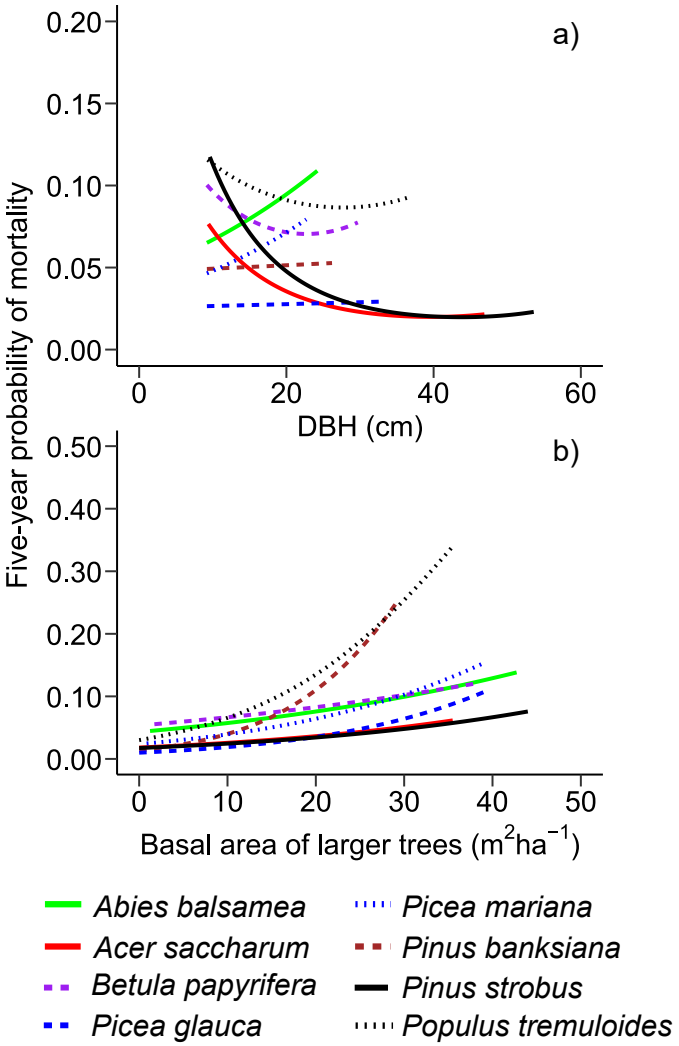

Figure 5: Predicted five-year probability of mortality in function of harvest occurrence during the interval. Other variables were set to their means as shown in Tables 1 and 2.